Lift Correlations from Direct Numerical Simulation of Solid-Liquid Flow

Daniel D. Joseph
Department of Aerospace Engineering and Mechanics, University of Minnesota
Minneapolis, MN 55455
(612) 625-0309 office; (612) 625-1558 fax
E-mail: *joseph@aem.umn.edu*
http://www.aem.umn.edu/Solid-Liquid_Flows

Abstract

Lift forces acting on a fluidized particle play a central role in many important applications, such as the removal of drill cuttings in horizontal drill holes, sand transport in fractured reservoirs, sediment transport and cleaning of particles from surfaces. The problem of lift is studied using direct numerical simulations. Lift formulas which respect the fact that the lift must change sign on either side of the "Segré-Silberberg" radius are discussed. An accurate analytical expression for the slip velocity of circular particles in Poiseuille flow is derived. We show that the lift-off of single particles and many particles in horizontal flows follow laws of similarity, power laws, which may be obtained by plotting simulation data on log-log plots.

1. Preface.

My collaborators on studies of lift are H. Choi, H. Hu, P. Huang, T. Ko, D. Ocando, N. Patankar and P. Singh. This is but one aspect of a concentrated NSF supported study of direct numerical simulations of solid-liquid flow. The results of such studies are collected at the project web site *http://www.aem.umn.edu/Solid-Liquid_Flows*. The whole field is reviewed in the monograph under preparation "Interrogation of Direct Numerical Simulations of Solid-Liquid Flow," which can be downloaded from the web site *http://www.aem.umn.edu/Solid-Liquid_Flows/papers/abs_Interrogation.html*.

2. Direct numerical simulation (DNS) of solid-liquid flow

. The current popularity of computational fluid dynamics is rooted in the perception that information implicit in the equations of fluid motion can be extracted without approximation using direct numerical simulation (DNS). A similar potential for solid-liquid flows, and multiphase flows generally, has yet to be fully exploited, even though such flows are of crucial importance in a large number of industries.

We have taken a major step toward the realization of this potential by developing two highly efficient parallel finite-element codes called *particle movers* for the direct numerical simulation of the motions of large numbers of solid particles in flows of Newtonian and viscoelastic fluids. One of the *particle movers* is based on moving unstructured meshes (arbitrary Lagranian-Eulerian or ALE) and the other on a structured mesh (distributed Lagrange multiplier or DLM) using a new method involving a distribution of Lagrange multipliers to ensure that the regions of space occupied by solids are in a rigid motion. Both methods use a new combined weak formulation in which the fluid and particle equations of motion are combined into a single weak equation of motion from which the hydrodynamic forces and torques on the particles have been eliminated. Several different kinds of code have been developed and tried on a variety of applications. See the project Web site, *http://aem.umn.edu/Solid-Liquid_Flows/*. To our knowledge we are the only group to compute fully resolved particulate flow at Reynolds numbers in the thousands occurring in the applications.

3. Richardson and Zaki (RZ) correlations.

The correlations of Richardson and Zaki (1954) (see also Pan, Joseph, Bai, Glowinski and Sarin 2001) are an empirical foundation for fluidized bed practice. They did very many experiments with different liquids, gases, particles and fluidization velocities. They plotted their data in log-log plots; miraculously this data fell on straight lines whose slope and intercept could be determined. This showed that the variables follow power laws; a theoretical explanation for this outstanding result has not been proposed. After processing the data Richardson and Zaki found that

$$V(\phi) = V(0)\,(1-\phi)^n$$

where $V(\phi)$ is the composite velocity which is the volume flow rate divided by the cross-section area at the distributor when spheres of volume fraction f are fluidized by drag. $V(0)$ is the "blow out" velocity, when $\phi = 0$; when $V > V(0)$ all the particles are blown out of the bed. Clearly $V(\phi) < V(0)$. The RZ exponent $n(R)$ depends on the Reynolds number $R = V(0)d/\nu$; $n = 2.39$ when $500 < R < 7000$.

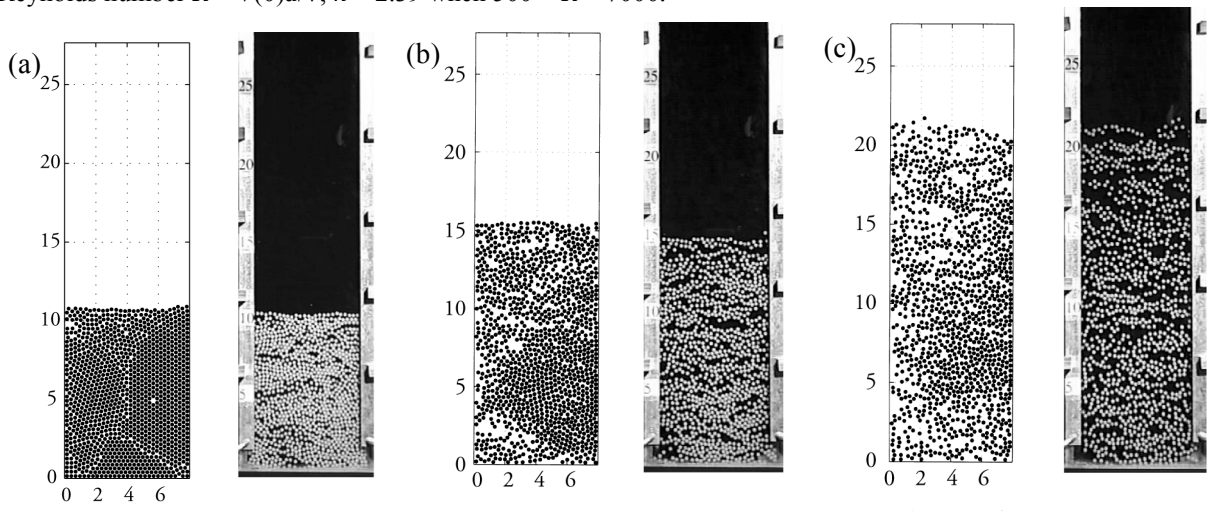

- V = 2 : Particle position at t = 5.625.
- The maximal particle Reynolds number is 1383.
- The maximal averaged particle Reynolds number is 130.

- V = 3.5 : Particle position at t = 17.238
- The maximal particle Reynolds number is 1671.
- The maximal avaraged particle Reynolds number is 236.

- V = 4.5 : Particle position at t = 31.
- The maximal particle Reynolds number is 1859.
- The maximal averaged particle Reynolds number is 292.

Figure 1. (Pan, Joseph, Bai, Glowinski and Sarin 2001). Snapshots of fluidization of 1204 spheres comparing experiment (right) and simulation (left) (a) V *= 2, (b)* V *= 3.5, (c)* V *= 4.5.*

We carried out DNS simulations of 1204 balls in a slit bed whose dimensions exactly match a real experiment. The simulation is compared with a matched real experiment and they give rise to essentially the same results (see figure 1). This simulation is presently at the frontier of DNS; it is a 3D computation of 1204 spheres at Reynolds numbers based on the sphere diameter of the order of 10^3 and the agreement with experiment is excellent. The details and animation of the computation (Pan, *et al* 2001) can be found at *http://www.aem.umn.edu/Solid-Liquid_Flows*.

The simulation of 1204 spheres was carried out in the bed [depth, width, height] = [0.686, 20.30, 70.22] cm. Snapshots comparing the animation with the experiment, in a frontal view are shown in figure 1. Figure 2 shows the fluidizing velocity vs. liquid fraction ε in a log-log plot; one line is for the simulation and another for the experiment. We draw a straight line with slop $n = 2.39$ through both sets of data. The fit is not perfect but we think rather encouraging. From the straight lines we determine the blow-out velocities $V_s(0) = 8.131$ cm/s for the simulation and $V_e(0) = 10.8$ cm/s for the experiment, and find the power laws

$$V_s(\phi) = 8.131\varepsilon^{2.39} \text{ cm/s}$$

and (1)

$$V_e(\phi) = 10.8\varepsilon^{2.39} \text{ cm/s}\ .$$

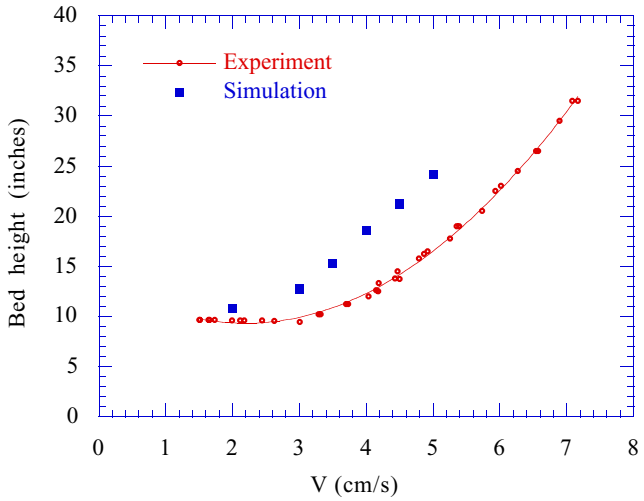

Figure 2(a). (Pan, et al 2001) The bed height vs. fluidizing velocity for both experiment and simulation.

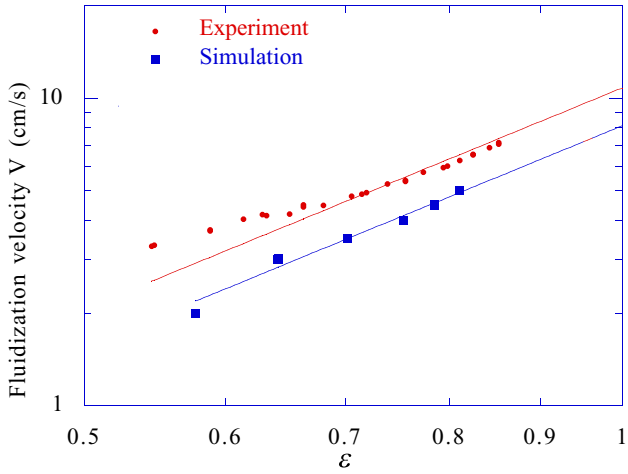

Figure 2(b). Data from Figure 2(a) plotted in a log-log plot. The slopes of the straight line are given by the Richardson-Zaki n = *2.39. The blow-out velocities* $V_s(0)$ *and* $V_e(0)$ *are defined as the intercepts at* $\varepsilon = 1$.

Pan, *et al* (2001) presented arguments that the discrepancy is due to the difference in the diameter 0.635cm of the sphere in the simulation and the average diameter 0.6398cm of the 1204 spheres uses in the experiments.

4. Single particle lift off and levitation to equilibrium

The problem of lift off and levitation to equilibrium of a single circular particle in a plane Poiseuille flow was simulated using an ALE particle mover in Patankar, Huang, Ko and Joseph (2001). The principal features of lift off and levitation to equilibrium are listed in the caption of figure 3. Heavier particles are harder to lift off. The critical lift off Reynolds number increases strongly with the density ratio. The height, velocity and angular velocity of the particle at equilibrium is given as a function of prescribed parameters in tables and trajectories from lift-off to equilibrium in graphs shown in Patankar, *et al* (2001).

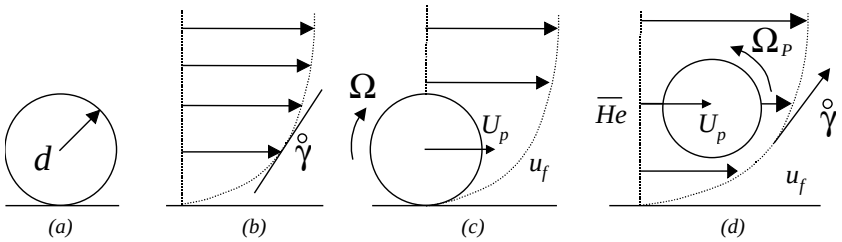

Figure 3. Lift off and levitation to equilibrium. The pressure gradient in the flow and on the particle is increased. The heavier than liquid particle slides and rolls on the bottom of the channel. At a critical speed the particle lifts off. It rises to a height in which the lift balances the buoyant weight. It moves forward without acceleration at a steady velocity and angular velocity.

The channel height is *W*, particle diameter *d*, density of fluid ρ_f and particle ρ_p, viscosity η, kinematic viscosity η/ρ_f . The equation of motion of fluid and particles made dimensionless with $[d,w,d/v,\eta\dot{\gamma}_w]$ where $\dot{\gamma}_w$ is the wall shear rate and $\overline{p}$ is the applied pressure gradient that drives the flow, are in the form

$$\textit{Solid}\ \begin{cases} R\left[\dfrac{\partial \mathbf{u}}{\partial t}+\mathbf{u}\cdot\nabla\mathbf{u}\right]=-\nabla p+2\dfrac{d}{w}\mathbf{e}_x+\nabla^2\mathbf{u}, & (2)\\ \dfrac{\rho_p}{\rho_f}R\dfrac{d\mathbf{U}}{dt}=-\dfrac{R_G}{R}e_y+2\dfrac{d}{w}\mathbf{e}_x+\dfrac{4}{\pi}\displaystyle\int_0^{2\pi}\left(-p+2\mathbf{D}[\mathbf{u}]\right)\cdot\mathbf{n}d\theta & (3)\\ \dfrac{\rho_p}{\rho_f}R\dfrac{d\mathbf{U}}{dt}=-\dfrac{R_G}{R}e_y+2\dfrac{d}{w}\mathbf{e}_x+\dfrac{4}{\pi}\displaystyle\int_0^{2\pi}\left(-p+2\mathbf{D}[\mathbf{u}]\right)\cdot\mathbf{n}d\theta\,. & (4)\end{cases}$$

The flow is determined by four dimensionless groups,

$$\frac{\rho_p}{\rho_f},\ \frac{2d}{w},\ R=\frac{\rho_f\,\dot{\gamma}_w\,d^2}{\eta},\ R_G=\frac{\rho_f\left(\rho_p-\rho_f\right)gd^2}{\eta^2} \qquad (5)$$

where *R* is the shear Reynolds number and R_G is a Reynolds number based on the sedimentation velocity in Stokes flow. The terms with the factor $\mathbf{e}_x$ come from the pressure gradient; the pressure gradient ($2d\mathbf{e}_x/w$ in (3)) drives the particle forward and the forward motion is resisted by the integral of the shear tractions.

Freely moving particles in steady flow have zero acceleration. The density ratio ρ_p/ρ_f vanishes when the particle accelerations are zero.

The critical value of the Reynolds number for lift-off increases with density of the particle from zero for neutrally buoyant $\rho_p = \rho_p$ circular particles to $R = 25$ for particles 1.4 times heavier than water $\rho_p = 1.4\,\rho_f$. After the particle lifts off it rises to an equilibrium height in which the buoyant weight equals the hydrodynamic lift. The equilibrium height for neutrally buoyant particles is called a "Segré-Silberberg" radius; it is determined by a balance of wall and shear gradient effects. The equilibrium height for heavy particles is lower than the Segré-Silberberg height. The rise to equilibrium is shown in figure 4.

DNS results given in Patankar, Huang, Ko and Joseph (2001) show that a circular particle will rise higher when the rotation of the particle is suppressed and least when the slip angular velocity is put to zero; the freely rotating zero torque case lies between. DNS allows such a comparison, which would be difficult or impossible to carry out in an experiment.

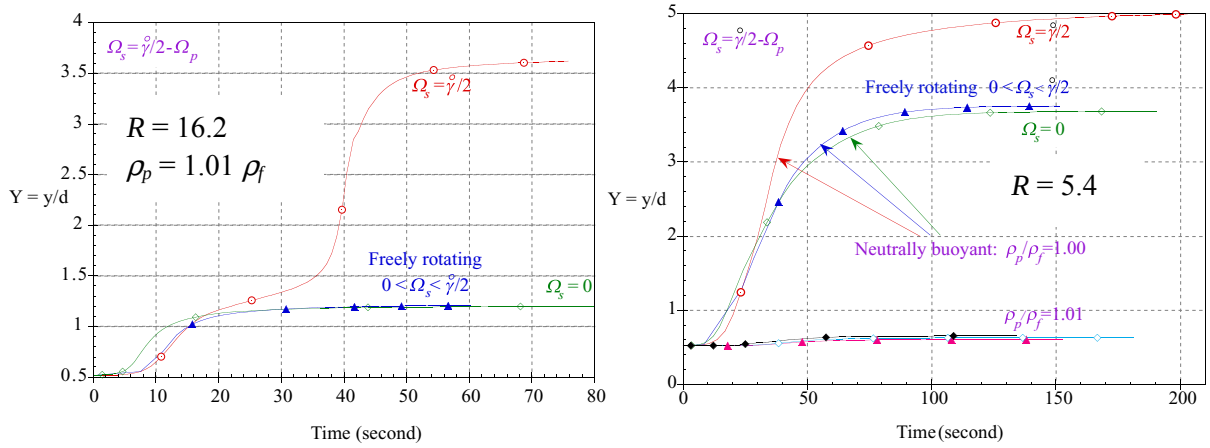

Figure 4. (Patankar, Huang, Ko and Joseph 2001.) Rise vs. time for R_w = 16.2 and 5.4. Compare rise of freely rotating and nonrotating particles. Nonrotating ones rise more. A neutrally buoyant, freely rotating particle rises closer to the center line than the "Segré-Silberberg" experiment; the nonrotating one rises even more. Models that ignore particle rotation overestimate lift. A yet smaller lift is obtained when the slip velocity is entirely suppressed ($\Omega_s = 0$), but the particle does rise. The greater the slip angular velocity, the higher the particle will rise.

5. Slip velocities, circulation and lift

In commercial packages for slurry flow in pipes, conduits and fractured oil and gas reservoirs, lift forces are not modeled, and in academic studies they are not modeled well. Possibly the best known and most used formula for lift is the Rayleigh Formula $L = \rho_f U \Gamma$ for aerodynamic lift. Here U is the forward velocity in still air that is produced by an external agent like a rocket engine, and Γ is the circulation, which is a complicated quantity determined by boundary layer separation. The lift on a free body in a shear flow is analogous and the lift formulas that have been proposed are in the form of U_s, the slip velocity, times $\rho_f \Gamma$, where Γ is a different quantity for different modelers. The slip velocity is the fluid velocity at the particle center when there is no particle minus the particle velocity. Since it is the fluid motion rather than an external agent which drives the motion of the particle, it might be expected that $U_s > 0$. Since free particles in shear flow migrate to an equilibrium radius, the associated Γ ought to change sign at this radius; in fact none of the lift formulas that have been proposed do change sign; if they are right at one side of the equilibrium they are wrong on the other. The slip angular velocity discrepancy defined as the difference between the slip angular velocity of a migrating particle and the slip angular velocity at its equilibrium position is positive below the position of equilibrium and negative above it. This discrepancy is the quantity that changes sign above and below the equilibrium position for neutrally buoyant particles, and also above and below the lower equilibrium position for heavy particles. On the other hand the slip velocity discrepancy U_s - U_{se} does not change sign Joseph, Ocando and Huang (2001).

6. Model of slip velocity

A long particle model was proposed in Joseph, Ocando and Huang (2001), which leads to an explicit expression for the particle velocity U_p of a circular particle in a Poiseuille flow. Referring to figure 5 we find that

$$U_A = \phi + \psi h_A d, \quad U_B = \phi + \psi h_B d \tag{6}$$

where

$$\phi = \frac{\bar{b}}{\eta}\left(2d + h_A + h_B\right)h_A h_B / 2\left(h_A + h_B\right)$$

$$\psi = \mathring{\gamma}\left(h_B + d/2\right) \Big/ 2\left(h_A + h_B\right)$$

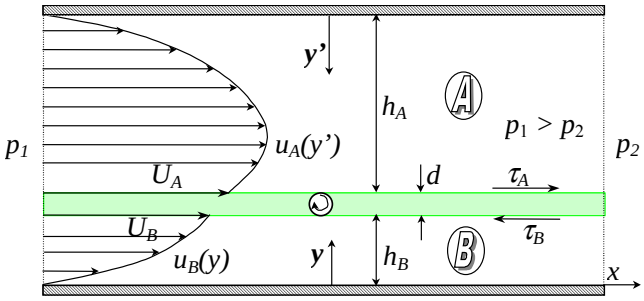

Figure 5. (Joseph, Ocando and Huang 2001.) The circular particle is replaced with a long rectangle where short side is d. The rectangle is so long that we may neglect the effects of the ends of the rectangle at sections near the rectangle's center. The rectangle is sheared at the shear rate of the circular particle $\Omega_p \cong \dot{\gamma}/2$ *(see figure 4). The velocity profile is Poiseuille flow on either side of the particle and* U_A *and* U_B *determined by requiring that the pressure gradient* $\overline{p}$ *balance the shear stress.*

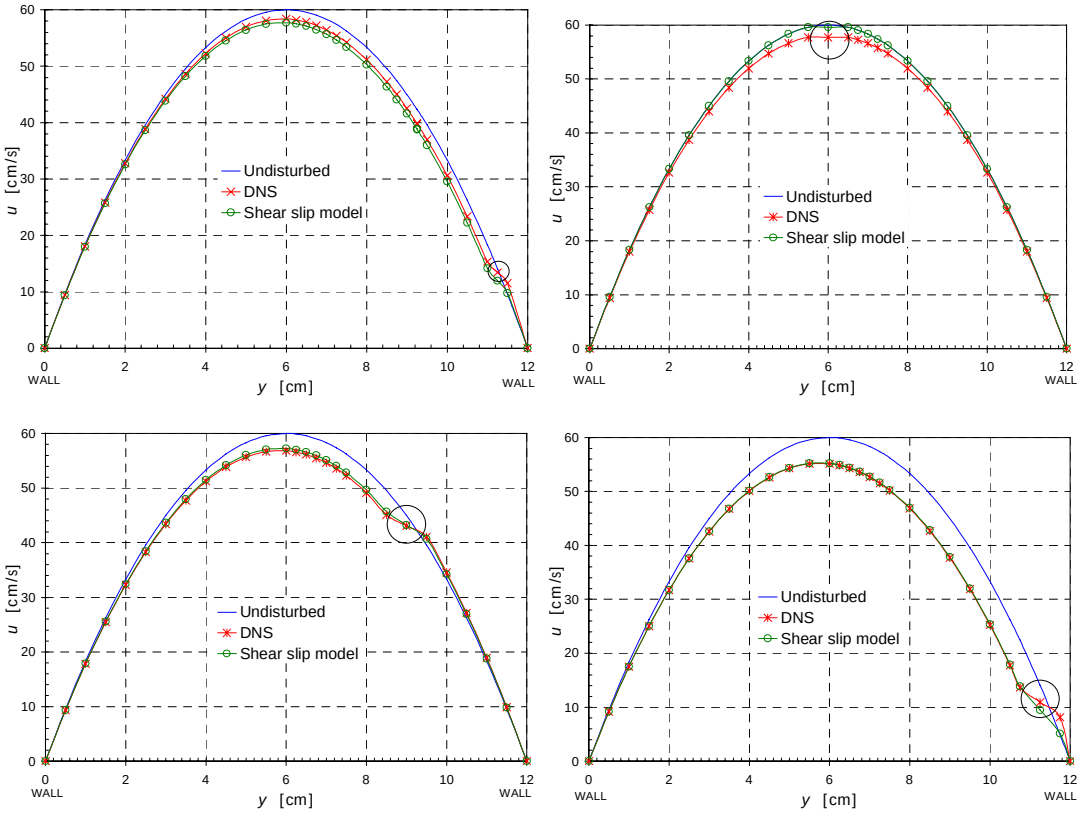

Figure 6. (Joseph, Ocando and Huang 2001.) Comparison of the velocity profiles (figure 5.) for the long particle model with the velocity profile on a line through the circular particle center computed by DNS for constrained motion at R = 20. In a constrained motion the y position of the particle is fixed, lateral motion is suppressed, but the particle is otherwise free to translate and rotate under the action of the hydrodynamic forces and torques.

and the particle velocity U_p is given by

$$U_p = \overset{\circ}{\gamma}\,(U_A + U_B)/2.$$

The slip velocity U_s is given by

$$U_s = \frac{\overline{p}}{2\eta}\left(h_B + \frac{d}{2}\right)\left(h_A + \frac{d}{2}\right) - U_p > 0 \quad \text{and} \quad U_s = 0 \quad \text{when} \quad d = 0. \tag{7}$$

A comparison of the velocity profile of the long particle model with the velocity profile through the center of the circular particle computed by direct numerical simulation is given in figure 6. Such a good agreement is surprising.

7. Bifurcation

A turning point bifurcation of steady forward flow of a single particle at equilibrium was found in direct simulations of rise trajectories reported in Choi and Joseph (2001); the height and particle velocity change strongly at such a point. A computational method advanced in Patankar, Huang, Ko and Joseph (2001) looks for the points on lift vs. height curve at which lift balances buoyant weight. This gives both stable and unstable solutions and leads to the "bifurcation" diagram shown in figure 7, which shows there are two turning points, hysteresis, but no new branch points.

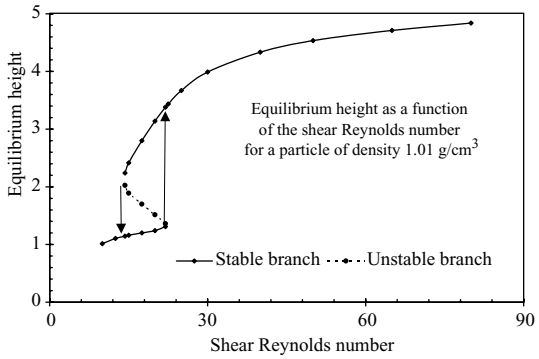

Figure 7. (Patankar, Huang, Ko and Joseph 2001.) Turning point "bifurcations" shown in the height vs. Reynolds number curve. There are two stable branches separated by an unstable branch.

Similar turning point bifurcations have been found also in computations of levitation to equilibrium of viscoelastic fluids of Oldroyd-B type. Similar instabilities have been found at yet higher Reynolds numbers. Bifurcations of sedimenting particles, including Hopf bifurcations to periodic motions, have been reported in the literature. It is probable that all the phenomena known for general dynamic systems occur also for particulate flows.

8. Levitation to equilibrium of 300 circular particles

The transport of a slurry of 300 heavier than liquid particles in a plane pressure driven flow was studied using DNS in Choi and Joseph (2001). Time histories of fluidization of the particles for three viscous fluids with viscosities η = 1, 0.2 and 0.01 (water) were computed at different pressure gradients. The study leads to the concept of fluidization by lift in which all the particles are suspended by lift forces against gravity perpendicular to the flow.

The time history of the rise of the mean height of particles at a given pressure gradient is monitored and the rise eventually levels off when the bed is fully inflated. The time taken for full inflation decreases as the pressure gradient (or shear Reynolds number) increases (see figure 8). At early times, particles are wedged out of the top layer by high pressure at the front and low pressure at the back of the particle in the top row (t = 1 in figure 8a, t = 0.9 in figure 8b).

The dynamic pressure at early times basically balances the weight of the particles in the rows defining the initial cubic array. This vertical stratification evolves into a horizontally stratified propagating wave of pressure, which tracks waves of volume fraction. The pressure wave is strongly involved in the lifting of particles. For low viscosity fluids like water where R_G is large the particle-laden region supports an "interfacial" wave corresponding to the wave of pressure. If R^2/R_G is large the interface collapses since the stronger lift forces push wave crests into the top of the channel, but the pressure waves persist (figure 9).

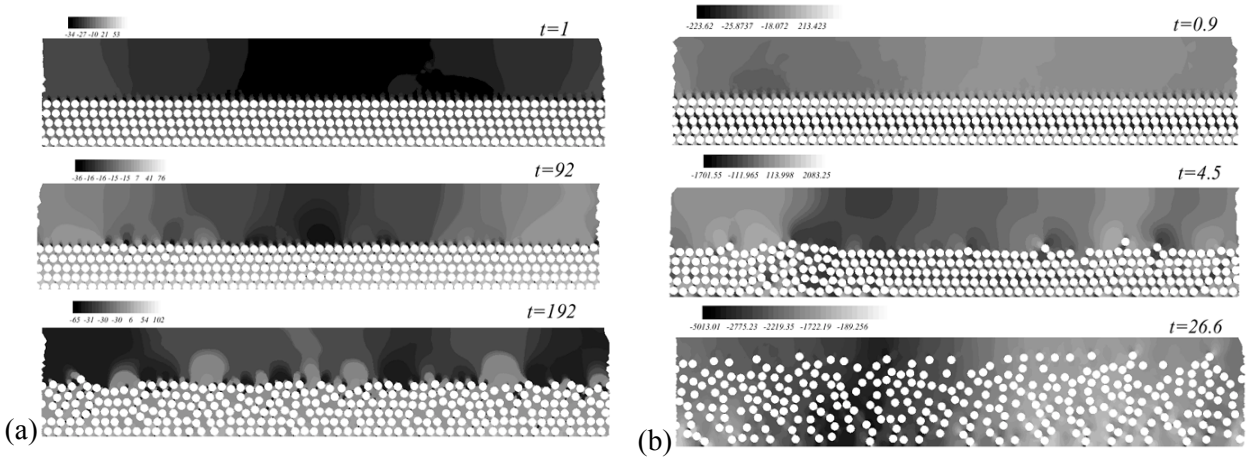

*Figure 8. (Choi and Joseph 2001.) (a) Snapshots of the fluidization of lift of 300 circular particles ρ_p = 1.01 g/cm^3 when η = 1 poise (*R = 5.4, R^2/R_G = 1.82*). The flow is from left to right. The gray scale gives the pressure intensity and dark is for low pressure. At early times particles are wedged out of the top layer by high pressure at the front and low pressure at the back of each and every circle in the top row. The vertical stratification of pressure at early times develops into a "periodic" horizontal stratification, a propagating pressure wave. The final inflated bed has eroded, rather tightly packed at the bottom with fluidized particles at the top. (b) Fluidization of 300 particles (*R = 120, R^2/R_G = 0.08*). The conditions are the same as in 9(a) but the ratio of lift to buoyant weight is greater and the fluidization is faster and the particle mass center rises higher than in the previous figures.*

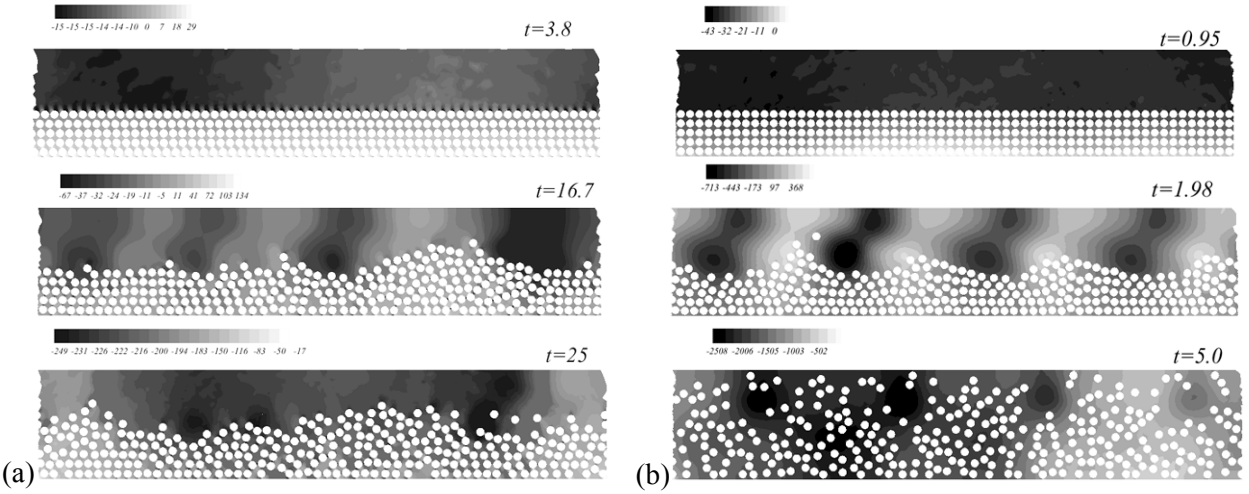

Figure 9. (Choi and Joseph 2001.) (a) Fluidization of 300 particles (η = 0.2 poise, R = 150, R^2/R_G = 1.63*). The final state of the fluidization at* t = 25 sec *has not fully eroded. The particles that lift out of the bed can be described as saltating. A propagating "interfacial" wave is associated with the propagating pressure wave at* t = 25*. (b). Fluidization of 300 particles (η = 0.2 poise,* R = 450, R^2/R_G =0.54*). The flow is from left to right. The particles can be lifted to the top of the channel.*

We did correlations in numerical experiments in 2D. Correlations work. We studied the levitation of 300 particles in a Poiseuille flow, Patankar, Ko, Choi and Joseph (2000), Choi and Joseph (2001), and created a data bank which when plotted on a log-log plot give rise to straight lines; this is to say that lift results for fluidized slurries are power laws in appropriate dimensionless parameters. This shows that fluidization of slurries by lift also falls into enabling correlations of the RZ type. The method of correlations is a link between direct simulation and engineering application.

Correlations allow generalizations from 20 or 30 data points into a continuum of points reaching even beyond where we can compute. Because you get so much from correlations even expensive calculations are cheap.

The correlation we found for lift-off of a single particle is in the form

$$R_G = aR^n, \quad a = 2.36, \qquad n = 1.39 \tag{8}$$

where R and R_G are defined by (5); a and n are obtained by plotting about 25 data points in a log R vs. log R_G plane (Patankar, Huang, Ko and Joseph (2001), figure 10). The straight lines that come out are amazing; they show that self-similarity lies at the foundation of solid-liquid flows. Similar correlations were found for lift-off in viscoelastic fluids Patankar, Ko and Joseph (2000), Patankar, *et al* (2001) (figure 11).

For 300 particles in Poiseuille flow we processed simulation data for the rise of the center of gravity of particles in the slurry; from the height rise we can compute the solid fraction ϕ. Processing data in log-log plots (figure 12) we got

$$R_G = 3.27 \times 10^{-4} (1-\phi)^{-9.05} R^{1.249} \tag{9}$$

This could be called a Richardson-Zaki type of correlation for fluidization by lift Patankar, Ko, Choi and Joseph (2001).

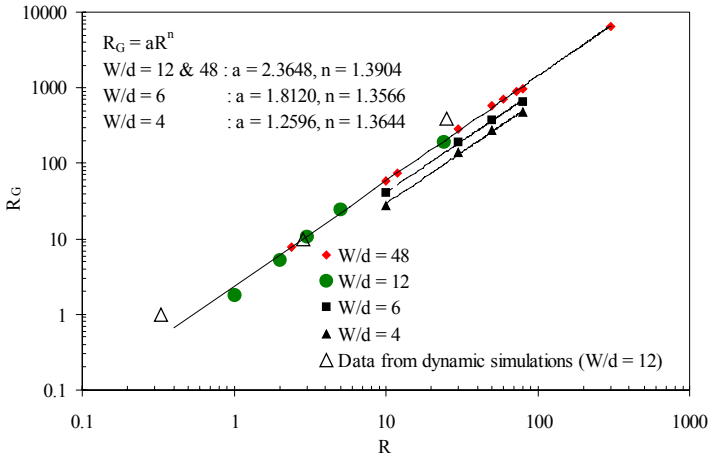

Figure 10. (Patankar, Huang, Ko and Joseph 2001.) The plot of R_G *vs. the critical shear Reynolds number* R *for lift-off on a logarithmic scale at different values of the channel width/diameter ratio* W/d*. This has evidently reached its asymptotic* W/d $\rightarrow \infty$ *value when* W/d = *12.*

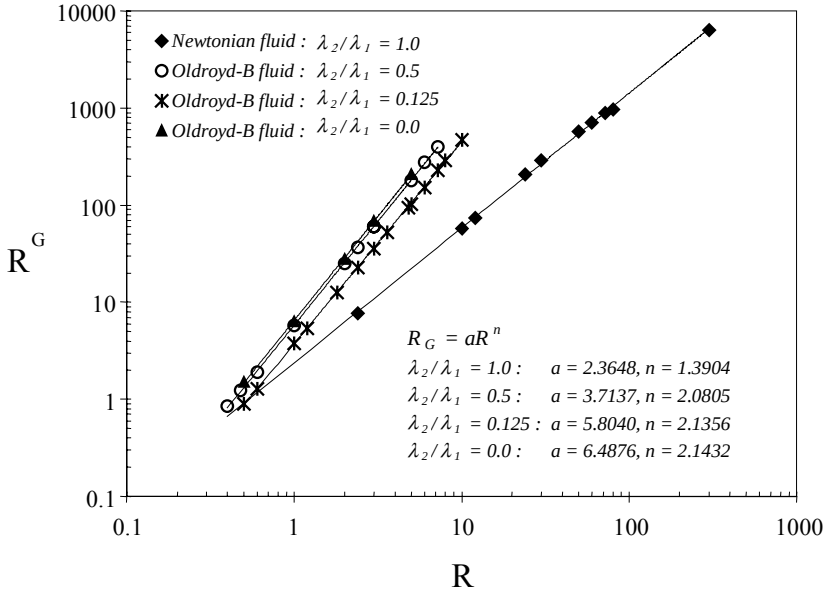

Figure 11. (Ko, Patankar and Joseph 2001.) RG vs. R for lift-off of an Oldroyd B fluid with different relaxation/ retardation time ratios in a log-log plot (W/d = 12, elasticity E = l1h/rfd2.)

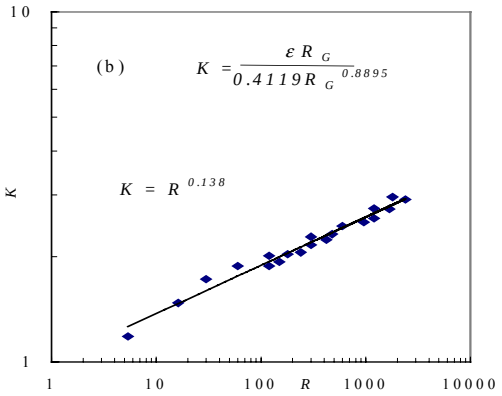

*Figure 12. (Patankar, Huang, Ko and Joseph 2001.) An engineering correlation (9) for lift-off from numerical simulations of 300 circular particles in plane Poiseuille flows of Newtonian fluids (*W/d = *12).*

9. Conclusions

We believe that research leading to optimal techniques of processing data for correlations from real and numerical experiments is founded on the far from obvious property of self similarity (power laws) in the flow of dispersions. The bases for this belief are the excellent correlations of experiments on fluidization and sedimentation done by Richardson and Zaki and the correlations for lifting of slurries in horizontal conduits obtained form numerical experiments described here. The method of correlations is a new link between DNS and engineering practice.

Results of two dimensional simulations of solid-liquid flows give rise to straight lines in log-log plots of the relevant dimensionless Reynolds numbers. The extent and apparent universality of this property is remarkable and shows that the flow of these dispersions are governed by a hidden property of self similarity leading to power laws. These power laws make a powerful connection between sophisticated high performance computation and the practical world of engineering correlations. The same methods for processing data are applied to numerical and real experiments.

The Richardson-Zaki correlation is of great relevance in seeing the image of the future. The power law in the RZ case is an example of what Barenblatt (1996) calls "incomplete self similarity" because the power itself depends on the Reynolds number, a third parameter. "Incomplete" self similarity might be generically expected of problems governed by three parameters and we expect to see it in the three dimensional simulations going forward.

Acknowledgment

This work was partially supported by the National Science Foundation DKI/New Computational Challenge grant (SNF/CTS 98-73236), by the DOE, Department of Basic Energy Sciences, by a grant from the Schlumberger foundation, from STIMLAB Inc. and by the Minnesota Supercomputer Institute.

References

Papers marked with ♦ have been written in the last year and have not yet been published; they can be found and downloaded from our web site, *http://www.aem.umn.edu/Solid-Liquid_Flows/references.html*.

G.I. Barenblatt 1996. *Scaling, Self Similarity and Intermediate Asymptotics*. Cambridge Univ. Press.

H.G. Choi and Daniel D. Joseph, 2001. Fluidization by lift of 300 circular particles in plane Poiseuille flow by direct numerical simulation, accepted by *J. Fluid Mech*. ♦

D.D. Joseph, D. Ocando and P.Y. Huang, 2001. Slip velocity and lift, accepted by *J. Fluid Mech*. ♦

T. Ko, N.A. Patankar and D.D. Joseph 2001. A note on the lift-off of a single particle in viscoelastic fluids. Submitted to *Phys. Fluids*.

N.A. Patankar, T. Ko, H.G. Choi and D.D. Joseph, 2001. A correlation for the lift-off of many particles in plan Poiseuille of Newtonian fluids, accepted by *J. Fluid Mech*. ♦

N.A. Patankar, P.Y. Huang, T. Ko and D.D. Joseph, 2001. Lift-off of a single particle in Newtonian and viscoelastic fluids by direct numerical simulation, accepted by *J. Fluid Mech.*.

T.-W. Pan, D.D. Joseph, R. Bai, R. Glowinski and V. Sarin, 2001. Fluidization of 1204 spheres: simulation and experiment, *J. of Fluid Mech*. to appear. ♦

J.F. Richardson and W.N. Zaki, 1954. Sedimentation and Fluidization: Part I, *Trans. Instn. Chem.* Engrs. **3**2, 35–53.